Brillouin Lasing in Ultra-High-Q Lithium Fluoride Disk Resonators

Souleymane Diallo, Guoping Lin, Romain Martinenghi, Luca Furfaro, Maxime Jacquot, and Yanne K. Chembo, *Senior Member, IEEE*

***Abstract*— We report the fabrication of an ultra-high-Q monolithic whispering gallery-mode resonator using a lithium fluoride crystal, with a quality factor above 10^8 at 1550 nm. We show that when pumped above a certain threshold, we can excite single Stokes Brillouin lasing in this resonator. We thereby demonstrate Brillouin lasing in a monofluoride crystal for the very first time, to the best of our knowledge. We provide a detailed theoretical investigation of Brillouin scattering in this resonator, using a time-domain model which tracks the dynamics of the Stokes and pump waves. We also perform a stability analysis which enables us to analytically determine the threshold pump power. We expect such crystalline Brillouin lasers to find potential applications for ultra-pure microwave and multi-wavelength generation, as well as for compact sensors.**

***Index Terms*— Lithium fluoride, Brillouin lasing, whispering gallery mode resonators.**

I. Introduction

WHISPERING-GALLERY mode (WGM) resonators are very interesting platforms as they can feature ultra-high Q factors and small mode volumes. These resonators permit to explore a very wide range of applications in photonics technology [1]–[4], and for this reason, they have attracted a large interest, such as for sensing, frequency comb generation and laser stabilization [5]–[10]. Light in such resonators is confined by total internal reflection with a photon lifetime that can be much longer than a microsecond. A very high light intensity can thereby build up in the torus-like eigenmodes of the resonator, located at its inner periphery. As a result, various nonlinear phenomena originating from the Raman [11], Brillouin [12]–[14], and Kerr effects [10], [15] are strongly enhanced and can be observed even with very low pump power.

Among these nonlinear effects, stimulated Brillouin scattering has one of the largest gain coefficients. It results from the interaction of a strong laser beam and acoustic phonons (lattice vibrations). The interaction is typically enabled by electrostriction, where a refractive index grating traveling with an acoustic wave velocity is formed. This grating can then scatter an incident photon into the backward direction with a Doppler downshift corresponding to the acoustic phonon frequency. The latter one can be calculated from the elastic constants of the material. Brillouin lasing for narrow linewidth lasers and low-phase-noise microwave oscillators have been recently demonstrated using silica WGM resonators [16]–[19]. However, to the best of our knowledge, Brillouin lasers based on crystalline WGM resonators have only been reported using calcium fluoride and barium fluoride crystals [12], [14].

Ultra-high-Q crystalline WGM resonators have been reported in several difluorides crystals [15], [21]–[23] using mechanical polishing techniques, but has been found to be a more difficult task with monofluoride ones [24]. In this letter, we report the fabrication of a monofluoride WGM resonator made of lithium fluoride (LiF) with a quality factor Q above 10^8 at the wavelength of 1550 nm. The quality factor has been measured using the cavity ring down spectroscopy technique [15], [21]. Brillouin lasing in the LiF resonator is demonstrated. We also propose a time-domain model for the forward and backward fields in order to track the dynamical behavior of these coupled waves. We perform a stability analysis of the corresponding set of coupled equations in order to determine the threshold power for Brillouin lasing. The key mechanisms of this phenomenon are thereby unveiled and the physical insights provided by the model are also discussed.

II. Fabrication and Characterization of the Ultra-High-Q LiF Disk-Resonator

Lithium fluoride is a cubic crystal with wide transparency window from the ultra-violet (UV) to mid-infrared (IR). In the UV range, it presents one of the highest transmission [25], thereby finding several applications in special UV optics but also in the X-ray domain. From a commercially available crystalline LiF WGM disk-resonator, we have used several steps of grinding and polishing to achieve a quality factor above 10^8, using an air-bearing spindle motor that spins the disc at high velocity [15], [20], [21]. During the grinding step, we used abrasives with decreasing grain size to shape the resonator rim into a sharp "V" geometrical form, needed to trap the intra-cavity photons. It should be mentionned that for a crystalline LiF WGM resonator, this step is relatively

Manuscript received September 28, 2015; revised January 4, 2016; accepted January 11, 2016. Date of publication January 25, 2016; date of current version March 17, 2016. This work was supported in part by the European Research Council through the Projects NextPhase and Versyt, in part by the Labex Action Project, in part by the Centre National d'Etudes Spatiales within the SHYRO Project, and in part by the Région de Franche-Comté.

The authors are with the Centre National de la Recherche Scientifique, Optics Department, Franche-Comté Electronique, Mécanique, Thermique et Optique - Sciences et Technologies Institute, University Bourgogne Franche-Comté, Besançon 25030, France (e-mail: souleymane.diallo@femto-st.fr; guoping.lin@femto-st.fr; romain.martinenghi@femto-st.fr; luca.furfaro@univ-fcomte.fr; maxime.jacquot@univ-fcomte.fr; yanne.chembo@femto-st.fr).

Color versions of one or more of the figures in this letter are available online at http://ieeexplore.ieee.org.

Digital Object Identifier 10.1109/LPT.2016.2521341

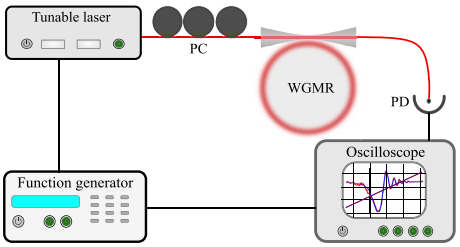

Fig. 1. Experimental setup for the WGM resonator characterization. PC: polarization controller; PD: photodiode; WGMR: whispering gallery mode resonator.

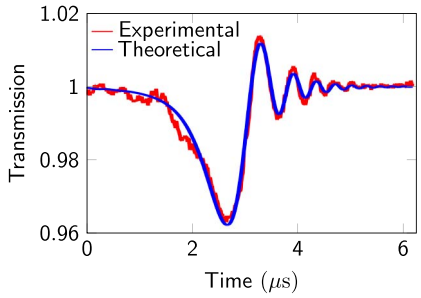

Fig. 2. Cavity ring-down timetrace. A theoretical fit gives an intrinsic quality factor of 3.3×10^8, an extrinsic quality factor of 2.58×10^8, and a loaded quality factor of 1.45×10^8 at 1550 nm.

fast (less than one hour) while it takes several hours for a MgF_2 WGM resonator. This grinding step is however delicate because of the low Mohs hardness of LIF, which is equal to 4. The second step consists in a repeated polishing procedure of the resonator rim using abrasive particles with a decreasing size down to 100 nm. Once the final polishing step is completed, we used white light vertical scanning interferometry to investigate the roughness of the resonator rim. This process consists of placing the resonator on a piezo-controlled stage and under a microscope equipped with a 40× magnification Mirau objective. A 3D reconstruction of the investigated area enables us to determine the surface roughness with great accuracy. For our LiF disk-resonator, we have measured a root-mean-square(rms) roughness of 11 nm.

We used the so-called cavity-ring-down measurement technique to determine the quality factor of the resonator. This technique is interesting because it can avoid the limitations due to laser linewidth and thermal effects. It also allows to obtain both intrinsic, extrinsic and loaded quality factors. It consists of a fast scan of the laser frequency across the resonance, and a measurement of the output timetrace which gives the pertinent information with regards to the loss mechanisms in the resonator. As illustrated in Fig. 1, a continuous wave laser with sub-kHz linewidth is swept at a scanning speed of 1.2 GHz/ms, and is used to couple light in the resonator through the evanescent field of a tapered silica fiber. The recorded transmission corresponds to the interference between the laser input and output signal from the disk-resonator. By fitting the experimental data of Fig. 2 with an analytical formula which is presented in ref. [26], we obtain at 1550 nm an intrinsic quality factor of 3.35×10^8, an extrinsic quality factor of 2.58×10^8 and a loaded quality factor of 1.45×10^8.

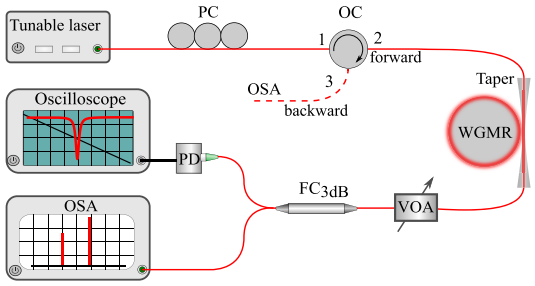

Fig. 3. The experimental setup for the WGM resonator characterization. PC: fiber polarization controller; L1, L2: GRIN lenses; VOA: Variable optical attenuator; FC_{3dB}: 3dB fiber coupler. PD: photodetector; OSA: Optical spectrum analyzer.

III. Brillouin Scattering in WGM Resonators

Stimulated Brillouin scattering is a nonlinear process resulting from the interaction between light and an acoustic wave. Since the acoustic wave travels at a given speed, the generation of the scattered wave is accompanied by a frequency shift due to the Doppler effect. Hence, a Stokes wave is generated when light and acoustic waves travel in the same direction and anti-Stokes wave is generated in the other case. Stimulated Brillouin scattering (SBS) is well known to be a power limiting factor in optical fiber communications. In fact, as the light power increases, the acoustic wave becomes stronger, and the optical fiber acts then as a Bragg mirror that is backscattering the injected power. The Brillouin effect can even be cascaded because many Stokes components may be sequentially generated even with very low pump power. Fiber Brillouin lasers feature linewidth narrowing effect where the Stokes line maybe narrower than the pump by a factor 10^4. Therefore, SBS can find application in several domains such as fiber lasers, microwave frequency generation, and rotation sensing. Brillouin lasing has been reported in several fluoride crystals such as calcium Fluoride ((CaF_2)) and barium fluoride ((BaF_2)). A narrow linewidth Brillouin microcavity laser and an ultra-low-phase-noise microwave synthetizer have also been demonstrated using chemically etched ultrahigh-Q-silica-on-silicon wedge resonators [19].

In this letter, we report Brillouin lasing at 1550 nm using a lithium fluoride resonator with a quality factor beyond one hundred millions. The pump and scattered signals are separated by a frequency shift $\nu_B = \Omega_B/2\pi = 2n_{eff}V_a/\lambda_L$ where n_{eff} is the effective refractive index of the WGM optical mode, λ_L is the optical wavelength of the laser in vacuum, and V_a the phase velocity of the acoustic wave. The latter is calculated using the following expression: $V_a = [(C_{11}+C_{12}+2C_{44})/2\rho]^{\frac{1}{2}}$ where $C_{11} = 1.3197 \times 10^{11}$ N.m^{-2}, $C_{12} = 0.4767 \times 10^{11}$ N.m^{-2}, and $C_{44} = 0.6364 \times 10^{11}$ N.m^{-2} represent the elastic constants of LiF, and $\rho = 2.639$ g.cm^{-3} his volumic mass. We therefore obtain an acoustic speed of $V_a = 7.62$ km.s^{-1} and a Brillouin frequency shift of $\nu_B = 13.61$ GHz.

We have designed an experimental setup in order to measure the spectra of the forward and backward waves, and it is displayed in Fig. 3. The measurements have provided evidence of Brillouin lasing as shown in Fig. 4, where the experimental Brillouin shift is in excellent agreement with the theoretically

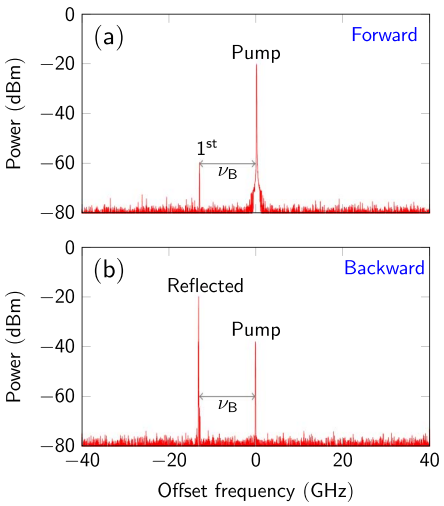

Fig. 4. Experimental spectra of the intra-cavity fields. The frequency ν_B corresponds to the Brillouin frequency shift. (a) Forward direction. (b) Backward direction. Note that the Brillouin signal in the forward direction and the pump signal in the backward direction are induced by parasitic Rayleigh backscattering.

predicted value ν_B. It should be noted that our WGM resonator features a transverse multimode structure. The Brillouin shift is in fact excited in a mode belonging to another eigenmode family with regards to the pump. In other words, if the pumped mode belongs to the eigenmode family $n = n_1$ (there are n_1 radial maxima of intensity), then the Brillouin-excited mode belongs to an eigenmode family $n_2 \neq n_1$. This is why it is possible to obtain Brillouin lasing in our crystalline WGM resonators even when the Brillouin shift does not match (a multiple of) the FSR. The demonstration of Brillouin lasing in LiF provides the possibility to generate new frequencies in microwave photonics applications using WGM resonators, since the Brillouin shift is material-specific. The other advantage of this crystal, already highlighted, is that it has an excellent transparency down to the deep ultra-violet, thereby allowing for applications in that wavelength range.

IV. Time-Domain Dynamics and Determination of the Threshold Pump Power

When the resonator is pumped with a resonant continuous-wave laser, Brillouin scattering can excite a backward wave [27]. Using a time-domain model, we can track the temporal dynamics of the forward and backward fields $\mathcal{F}(t)$ and $\mathcal{B}(t)$ using the following equations:

$$\frac{d\mathcal{F}}{dt} = -\frac{1}{2}\Delta\omega_{\text{tot}}\mathcal{F} + i\sigma_{\text{f}}\mathcal{F} - \frac{g_{\text{B}}v_g}{2A_{\text{eff}}}|\mathcal{B}|^2\mathcal{F} + \sqrt{\Delta\omega_{\text{ext}}/T_{\text{R}}}\sqrt{P} \quad (1)$$

$$\frac{d\mathcal{B}}{dt} = -\frac{1}{2}\Delta\omega_{\text{tot}}\mathcal{B} + i\sigma_{\text{b}}\mathcal{B} + \frac{g_{\text{B}}v_g}{2A_{\text{eff}}}|\mathcal{F}|^2\mathcal{B}, \quad (2)$$

where P is the imput pump power in watts. The loaded linewidth $\Delta\omega_{\text{tot}} = \omega_{\text{c}}/\text{Q}_{\text{tot}}$ is the sum of the intrinsic linewidth $\Delta\omega_{\text{in}} = \omega_{\text{c}}/Q_{\text{in}}$ and extrinsic (or coupling) linewidth $\Delta\omega_{\text{ext}} = \omega_{\text{c}}/Q_{\text{ext}}$, where $Q_{\text{tot}}^{-1} = Q_{\text{in}}^{-1} + Q_{\text{ext}}^{-1}$, $T_{\text{R}} = \pi D/v_g$ represent the cavity round-trip time, $g_{\text{B}} \sim 10^{-11}$ m/W is the Brillouin gain of the material, v_g is the group velocity of the intra-cavity optical signals and $A_{\text{eff}} \sim D^{\frac{5}{6}}\lambda_{\text{L}}^{\frac{7}{6}}$ the effective cross-sectionnal area of the pumped eigenmode in the disk-resonator. D is the diameter of the resonator. The parameters σ_{f} and σ_{b} are cavity detuning parameters between the fields and the cold-cavity resonances. For the sake of simplicity, they are uniformly set to zero in this work and we assume the laser frequency ω_{L} is equal to the resonance frequency ω_{c} of the pumped mode. It should be noted that in this simplified model, the build-up of the acoustic wave has been neglected and it is assumed that the phonon field adiabatically follows the photon fields.

The above equations enable us to determine analytically the threshold power P_{th} needed to trigger Brillouin lasing. The starting point is to find the fixed point of the system below threshold, which is obtained by setting all the derivatives to zero, and setting $\mathcal{B} \equiv 0$ (no backward field). We find the stationary intra-cavity forward and backward fields are explicitly defined as

$$\mathcal{F}_{\text{st}} = 2\frac{\sqrt{\Delta\omega_{\text{ext}}/T_{\text{R}}}}{\Delta\omega_{\text{tot}}}\sqrt{P} \quad (3)$$

$$\mathcal{B}_{\text{st}} = 0. \quad (4)$$

We can now perturb this trivial equilibrium and check if this perturbation exponentially increases (onset of Brillouin scattering) or decays (in this case, the trivial fixed point is stable). The forward field is perturbed as $\mathcal{F} = \mathcal{F}_{\text{st}} + \delta\mathcal{F}$, yielding a square modulus $|\mathcal{F}|^2 \simeq |\mathcal{F}_{\text{st}}|^2 + \mathcal{F}_{\text{st}}\delta\mathcal{F}^* + \mathcal{F}_{\text{st}}^*\delta\mathcal{F}$ when the higher-order perturbation $|\delta\mathcal{F}|^2$ is neglected. On the other hand, the backward field is perturbed as $\mathcal{B} = \mathcal{B}_{\text{st}} + \delta\mathcal{B} \equiv \delta\mathcal{B}$, which has a null square modulus in a first-order approximation. By inserting these perturbed variables in Eqs. (1) and (2), we obtain the following linear flow

$$\delta\dot{\mathcal{F}} = -\frac{1}{2}\Delta\omega_{\text{tot}}\delta\mathcal{F} \quad (5)$$

$$\delta\dot{\mathcal{B}} = \left[-\frac{1}{2}\Delta\omega_{\text{tot}} + \frac{g_{\text{B}}v_g}{2A_{\text{eff}}}|\mathcal{F}_{\text{st}}|^2\right]\delta\mathcal{B}. \quad (6)$$

It appears that the perturbations of the forward and backward fields are uncoupled. In fact, the forward field perturbation always decays, while on the other hand, the backward field is excited when the Brillouin gain overcomes the losses, that is, when

$$\frac{g_{\text{B}}v_g}{2A_{\text{eff}}}|\mathcal{F}_{\text{st}}|^2 > \frac{1}{2}\Delta\omega_{\text{tot}}. \quad (7)$$

Using Eq. (3) with the above equation, it can finally be shown that the threshold power to trigger Brillouin lasing is explicitly expressed as

$$P_{\text{th}} = \omega_{\text{L}}^2\frac{Q_{\text{ext}}}{Q_{\text{tot}}^3}\frac{A_{\text{eff}}T_{\text{R}}}{4g_{\text{B}}v_g} \propto \frac{1}{g_{\text{B}}}\frac{V_{\text{eff}}}{Q_{\text{tot}}^2}, \quad (8)$$

with $V_{\text{eff}} = 2\pi a A_{\text{eff}}$ being the mode volume. A low threshold pump power therefore requires a high Brillouin gain, a high loaded quality factor, and a small mode volume. It is noteworthy that the formula proposed in Eq. (8) corresponds to the one proposed in ref. [12] for the case of critical coupling.

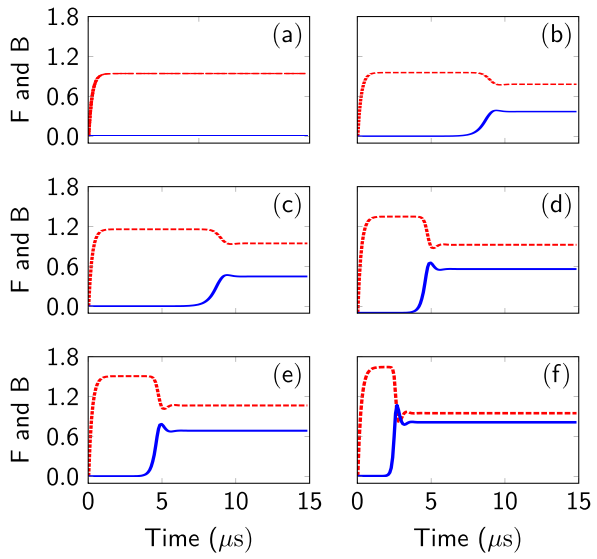

Fig. 5. Numerical simulation for the temporal dynamics of the forward field $\mathcal{F}(t)$ (red dashed line) and backward field $\mathcal{B}(t)$ (continuous blue line). The values or the input pump power is increased a follows: (a) $P = 0.99 \times P_{\text{th}}$; (b) $P = 1.01 \times P_{\text{th}}$; (c) $P = 1.5 \times P_{\text{th}}$; (d) $P = 2 \times P_{\text{th}}$; (e) $P = 2.5 \times P_{\text{th}}$; (f) $P = 3 \times P_{\text{th}}$.

However, we have experimentally found that the threshold power was systematically in the mW range, as for BaF_2 [21].

The results of the numerical simulation are displayed in Fig. 5, and we have used the following physical parameters: $D = 12$ mm, $A_{\text{eff}} = 1.0 \times 10^{-11}$ m^2, $n_{\text{eff}} = 1.38$, $Q_{\text{tot}} = 1.45 \times 10^8$, $Q_{\text{in}} = 3.35 \times 10^8$, $Q_{\text{ext}} = 2.58 \times 10^8$, and $\omega_{\text{L}} = 2\pi\, c/\lambda_{\text{L}} = 2\pi \times 192.6$ THz, We observe that below the threshold pump power, the backscattered field is not excited. However, when $P > P_{\text{th}}$, Brillouin lasing is triggered and the backward field builds up faster as the pump power is higher. The permanent regime is reached within ten microseconds, which corresponds to few photon lifetimes $\tau_{\text{ph}} = 1/\Delta\omega_{\text{tot}}$.

V. Conclusion

We have reported a LiF WGM resonator with an intrinsic quality factor of three hundred million at telecom wavlength. We have also demonstrated the excitation of a Stokes wave with this resonator, thereby evidencing for the first time Brillouin lasing in a monofluoride cristal, to the best of our knowledge. We have proposed a set of coupled nonlinear equations to investigate the dynamics of the forward and backward fields, and we have performed a stability analysis which enabled us to determine analytically the threshold pump power. Further research will be devoted to the exploration of the various applications that can be powered by this phenomenon, with an emphasis on ultra-stable microwave generation.

References

[1] A. B. Matsko, A. A. Savchenkov, D. Strekalov, V. S. Ilchenko, and L. Maleki, "Review of applications of whispering-gallery mode resonators in photonics and nonlinear optics," *IPN Prog. Rep.*, vol. 42, no. 162, pp. 1–51, Aug. 2005.

[2] V. S. Ilchenko and A. B. Matsko, "Optical resonators with whispering-gallery modes—Part II: Applications," *IEEE J. Sel. Topics Quantum Electron.*, vol. 12, no. 1, pp. 15–32, Jan./Feb. 2006.

[3] A. B. Matsko and V. S. Ilchenko, "Optical resonators with whispering-gallery modes—Part I: Basics," *IEEE J. Sel. Topics Quantum Electron.*, vol. 12, no. 1, pp. 3–14, Jan./Feb. 2006.

[4] A. Chiasera *et al.*, "Spherical whispering-gallery-mode microresonators," *Laser Photon. Rev.*, vol. 4, no. 3, pp. 457–482, pp. 2010.

[5] A. A. Savchenkov, E. Rubiola, A. B. Matsko, V. S. Ilchenko, and L. Maleki, "Phase noise of whispering gallery photonic hyper parametric microwave oscillators," *Opt. Exp.*, vol. 16, no. 6, pp. 4130–4144, Mar. 2008.

[6] Y. Deng, F. Liu, Z. C. Leseman, and M. Hossein-Zadeh, "Thermo-optomechanical oscillator for sensing applications," *Opt. Exp.*, vol. 21, no. 4, pp. 4653–4664, Feb. 2013.

[7] M. C. Collodo, F. Sedlmeir, B. Sprenger, S. Svitlov, L. J. Wang, and H. G. L. Schwefel, "Sub-kHz lasing of a CaF_2 whispering gallery mode resonator stabilized fiber ring laser," *Opt. Exp.*, vol. 22, no. 16, pp. 19277–19283, Aug. 2014.

[8] A. A. Savchenkov, A. B. Matsko, V. S. Ilchenko, N. Yu, and L. Maleki, "Whispering-gallery-mode resonators as frequency references. II. Stabilization," *J. Opt. Soc. Amer. B*, vol. 24, no. 12, pp. 2988–2997, Dec. 2007.

[9] F. Vollmer and S. Arnold, "Whispering-gallery-mode biosensing: Label-free detection down to single molecules," *Nature Methods*, vol. 5, no. 7, pp. 591–596, Jul. 2008.

[10] T. Herr *et al.*, "Universal formation dynamics and noise of Kerr-frequency combs in microresonators," *Nature Photon.*, vol. 6, pp. 480–487, Jun. 2012.

[11] I. S. Grudinin and L. Maleki, "Efficient Raman laser based on a CaF_2 resonator," *J. Opt. Soc. Amer. B*, vol. 25, no. 4, pp. 594–598, Mar. 2008.

[12] I. S. Grudinin, A. B. Matsko, and L. Maleki, "Brillouin lasing with a CaF_2 whispering gallery mode resonator," *Phys. Rev. Lett*, vol. 102, no. 4, pp. 043902-1–043902-4, Jan. 2009.

[13] M. Tomes and T. Carmon, "Photonic micro-electromechanical systems vibrating at X-band (11-GHz) rates," *Phys. Rev. Lett.*, vol. 102, no. 11, pp. 113601-1–113601-4, Mar. 2009.

[14] G. Lin *et al.*, "Cascaded Brillouin lasing in monolithic barium fluoride whispering gallery mode resonators," *Appl. Phys. Lett.*, vol. 105, no. 23, p. 231103, 2014.

[15] R. Henriet *et al.*, "Kerr optical frequency comb generation in strontium fluoride whispering-gallery mode resonators with billion quality factor," *Opt. Lett.*, vol. 40, no. 7, pp. 1567–1570, Apr. 2015.

[16] H. Lee *et al.*, "Chemically etched ultrahigh-Q wedge-resonator on a silicon chip," *Nature Photon.*, vol. 6, no. 6, pp. 369–373, May 2012.

[17] Z. Ou, X. Bao, Y. Li, B. Saxena, and L. Chen, "Ultranarrow linewidth Brillouin fiber laser," *IEEE Photon. Technol. Lett.*, vol. 26, no. 20, pp. 2058–2061, Oct. 15, 2014.

[18] K. Saleh, P. Merrer, O. Llopis, and G. Cibiel, "Millimeter wave generation using Brillouin scattering in a high Q fiber ring resonator," in *Proc. Int. Topical Meeting Microw. Photon. (MWP)*, Sep. 2012, pp. 164–167.

[19] J. Li, H. Lee, and K. J. Vahala, "Microwave synthesizer using an on-chip Brillouin oscillator," *Nature Commun.*, vol. 4, no. 2097, pp. 1–7, Jun. 2013.

[20] H. Tavernier, P. Salzenstein, K. Volyanskiy, Y. K. Chembo, and L. Larger, "Magnesium fluoride whispering gallery mode disk-resonators for microwave photonics applications," *IEEE Photon. Technol. Lett.*, vol. 22, no. 22, pp. 1629–1631, Nov. 15, 2010.

[21] G. Lin, S. Diallo, R. Henriet, M. Jacquot, and Y. K. Chembo, "Barium fluoride whispering-gallery-mode disk-resonator with one billion quality-factor," *Opt. Lett.*, vol. 39, no. 20, pp. 6009–6012, Oct. 2014.

[22] A. A. Savchenkov, V. S. Ilchenko, A. B. Matsko, and L. Maleki, "Kilohertz optical resonances in dielectric crystal cavities," *Phys. Rev. A*, vol. 70, no. 5, pp. 051804-1–051804-4, Nov. 2004.

[23] A. A. Savchenkov, A. B. Matsko, V. S. Ilchenko, and L. Maleki, "Optical resonators with ten million finesse," *Opt. Exp.*, vol. 15, no. 11, pp. 6768–6773, May 2007.

[24] R. Henriet, A. Coillet, K. Saleh, L. Larger, and Y. K. Chembo, "Barium fluoride and lithium fluoride whispering-gallery mode resonators for photonics applications," *Opt. Eng.*, vol. 53, no. 7, pp. 071821-1–071821-3, Jul. 2014.

[25] M. J. Weber, *Handbook of Optical Materials*, vol. 19. Boca Raton, FL, USA: CRC Press, 2002, p. 043828.

[26] Y. Dumeige, S. Trebaol, L. Ghişa, T. K. Nguyên, H. Tavernier, and P. Féron, "Determination of coupling regime of high-Q resonators and optical gain of highly selective amplifiers," *J. Opt. Soc. Amer. B*, vol. 25, no. 12, pp. 2073–2080, Dec. 2008.

[27] G. P. Agrawal, *Nonlinear Fiber Optics*, vol. 5. New York, NY, USA: Academic, 2003, pp. 1–629.